

Pedro Alvim de Azevedo Santos

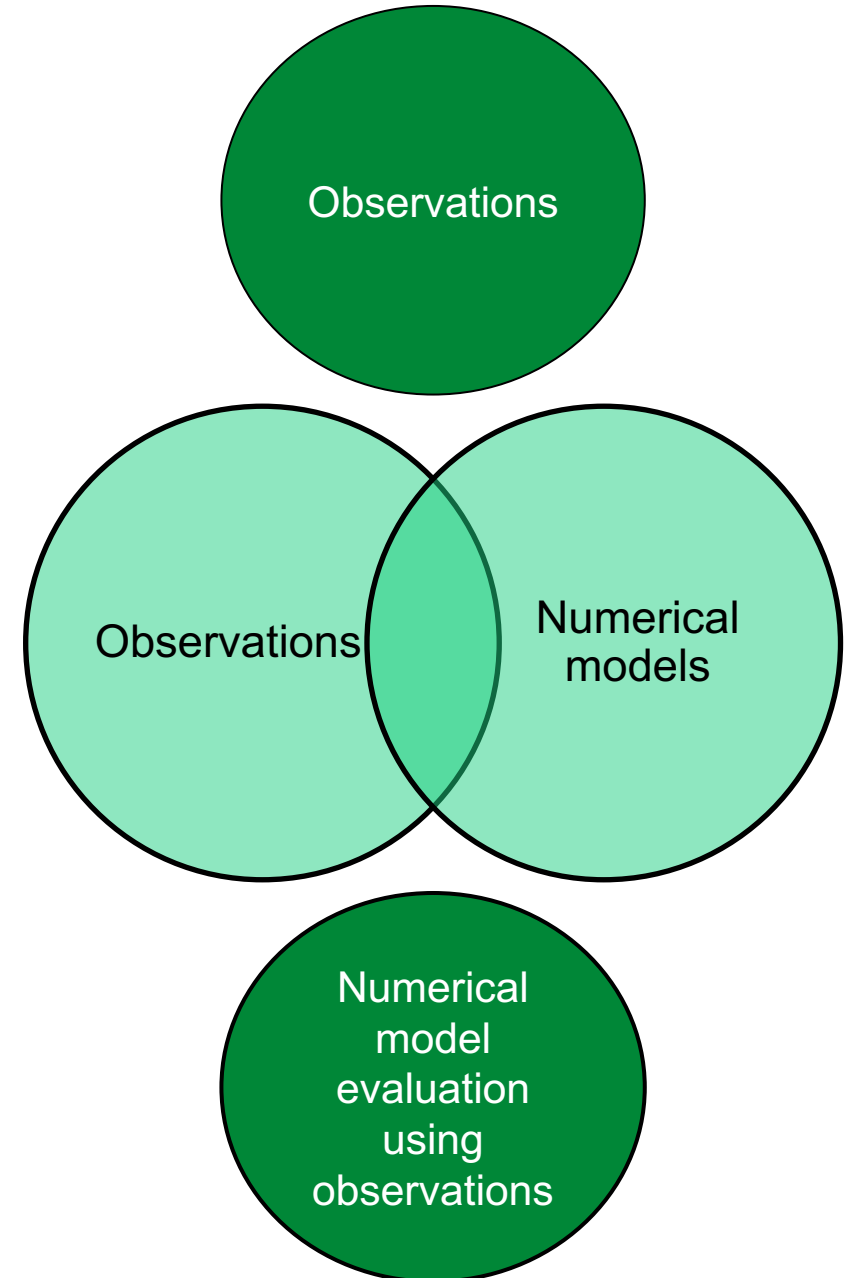
April 28th 2021

Untangling atmospheric flows through the lenses of wind lidars



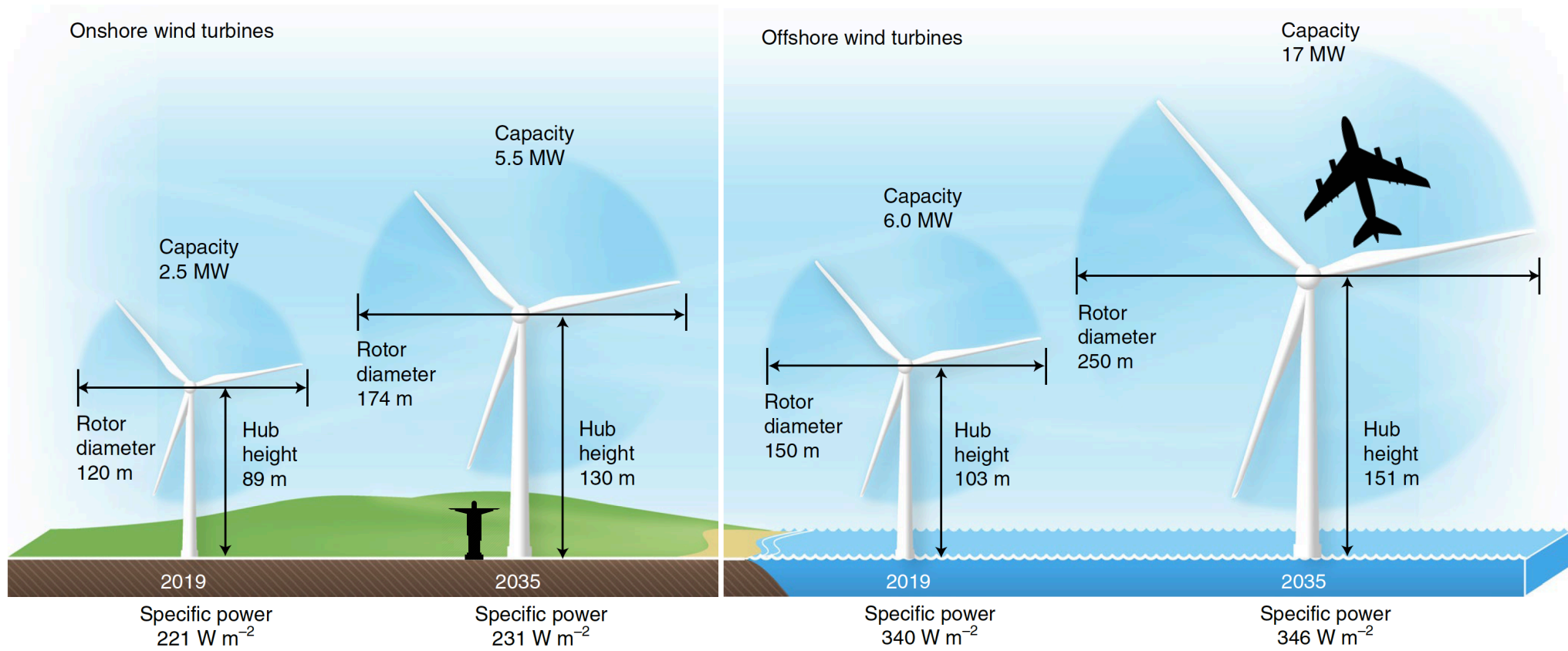
Agenda

- Motivation
- Background
- Hypotheses
- Alaiz measurement campaign
- An atmospheric hydraulic jump at Alaiz
- *K*-theory departure in the boundary layer
- Conclusions



Motivation - Wind energy scaling up

- Wind provided 4.7% of world's electricity in 2018. By 2050 is expected that wind energy will represent 31% of total electricity production (DNV, [2020](#)).
- Onshore wind >> complex terrain, offshore wind >> tall wind profiles



Source: Wiser et al., *Nature Energy* ([2021](#))

Motivation – Tall wind profile and large-scale effects

- Modern wind turbines occupy a large portion of the atmospheric boundary layer (ABL)
- Grand challenges of Wind Energy
 “mastering the physics of [wind] resource across scales” (Veers et al., [2019](#)).

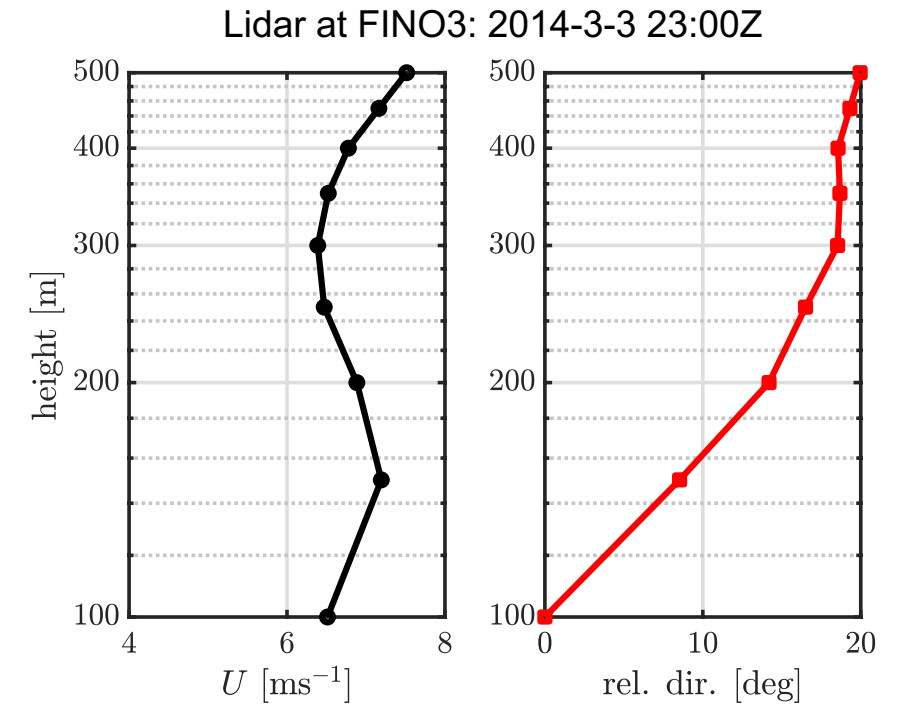
- This thesis will focus on:

Onshore

Offshore

Tall wind profile behavior

Large-scale atmospheric phenomena due to terrain interaction



Motivation – Tall wind profile and large-scale effects

- Modern wind turbines occupy a large portion of the atmospheric boundary layer (ABL)
- Grand challenges of Wind Energy
“mastering the physics of [wind] resource across scales” (Veers et al., [2019](#)).
- This thesis will focus on:

Onshore

Offshore

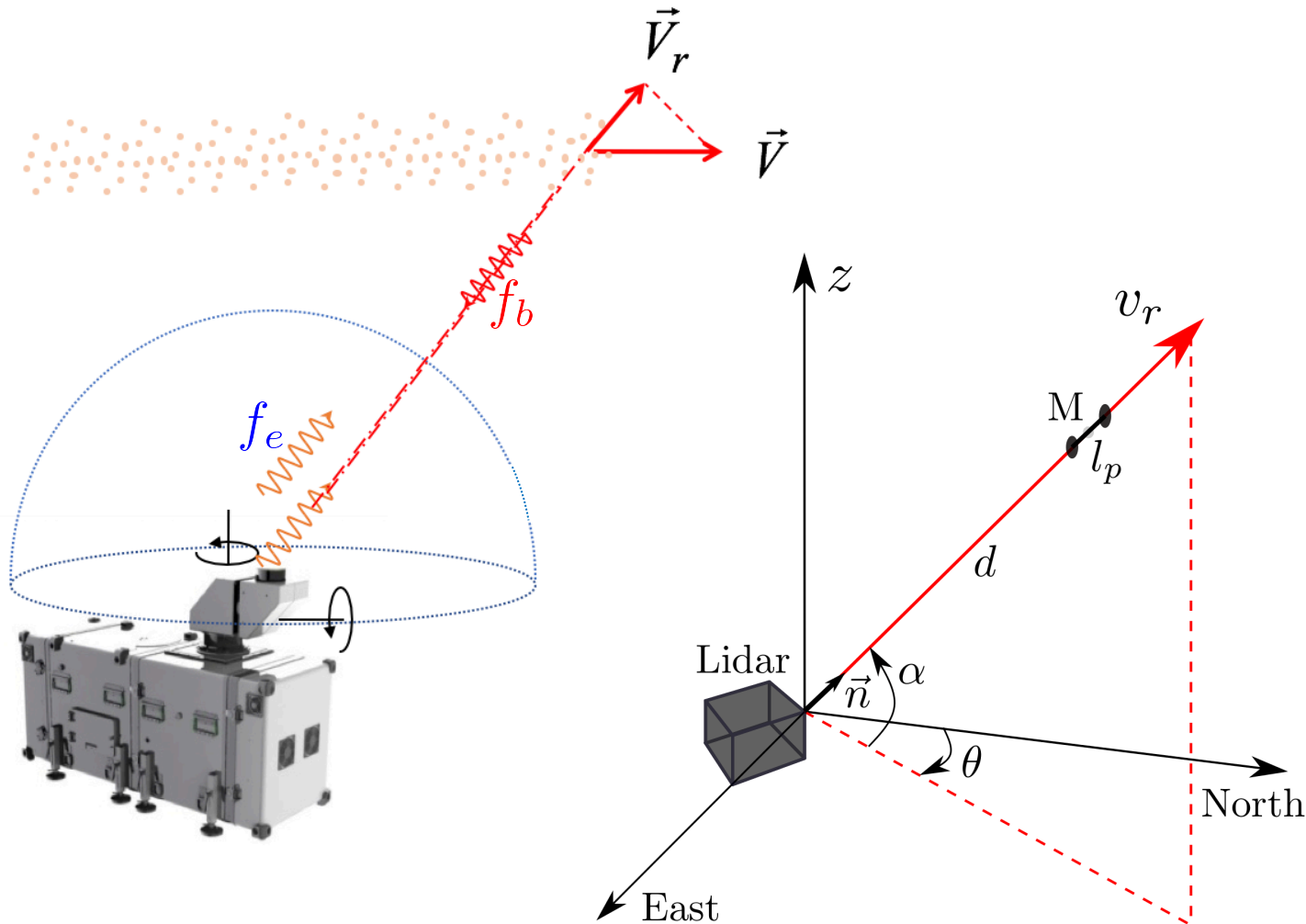
Tall wind profile behavior

Large-scale
atmospheric
phenomena due to
terrain interaction



Photo: Wobben Wind Power (José F. S. Neto & Thomás V. S. Araújo)

Lidars – *de facto* technology for remote wind sensing



Radial wind speed from Doppler shift:

$$\Delta f = f_b - f_e = \frac{2f_e}{c} v_r$$

Radial speed as projection of wind vector,

$$v_r(d, l_p, \alpha, \theta) = \vec{n} \cdot \vec{V}(\vec{n}, d)$$

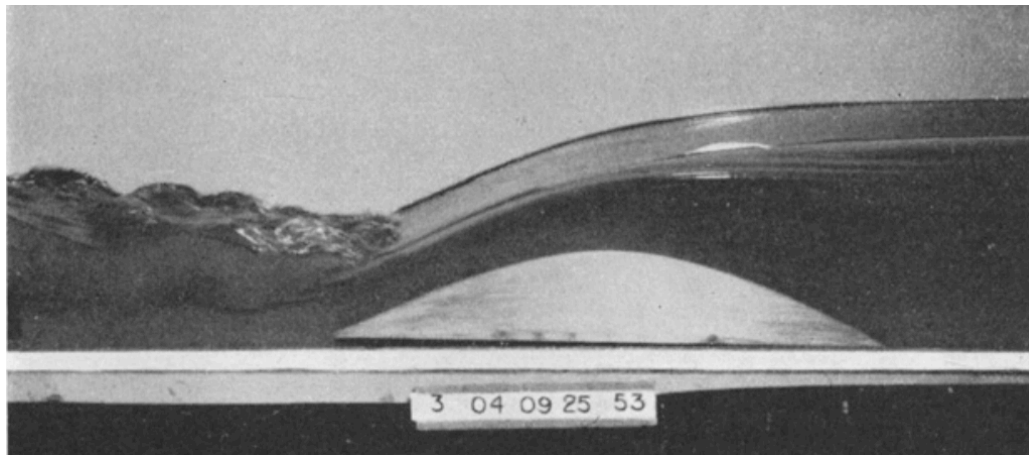
where,

$$\vec{n}(\theta, \alpha) = (\sin \theta \cos \alpha, \cos \theta \cos \alpha, \sin \alpha)$$

Flow over mountainous terrain

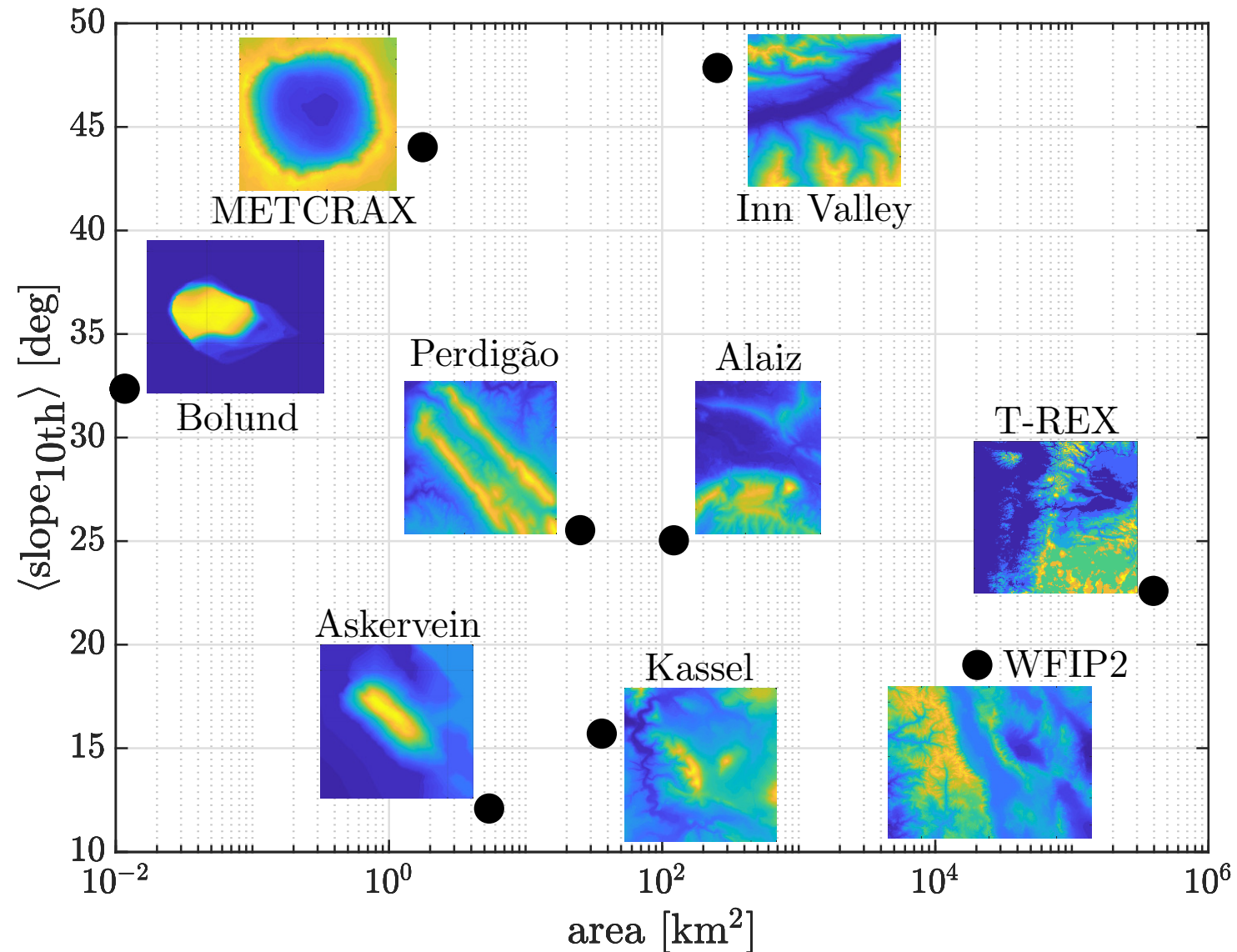
- When the topography has an elevation difference in order of the PBL height, Kaimal and Finnigan (1994) argue that buoyancy effects are significant to characterize the flow at all times.
- Brunt-Väisälä frequency (N) and Froude number (Fr) are two important parameters,

$$Fr_L = \frac{U}{NL} \qquad N = \sqrt{\frac{g}{\bar{\theta}} \frac{\partial \bar{\theta}}{\partial z}}$$

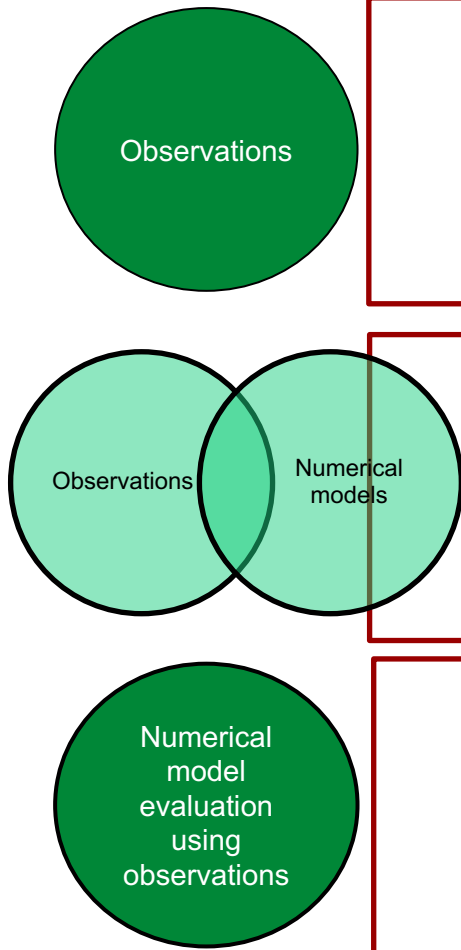


Source: Long (1954, *Tellus*)

Panorama of observations and model evaluation



Hypotheses



Observations

Hypothesis 1:

- Multi-lidar measurements of the mean wind flow **portray** flow patterns of different scales, such as atmospheric mountain waves and recirculation zones with features from 100 m and 10 km in mountainous terrain

Hypothesis 2:

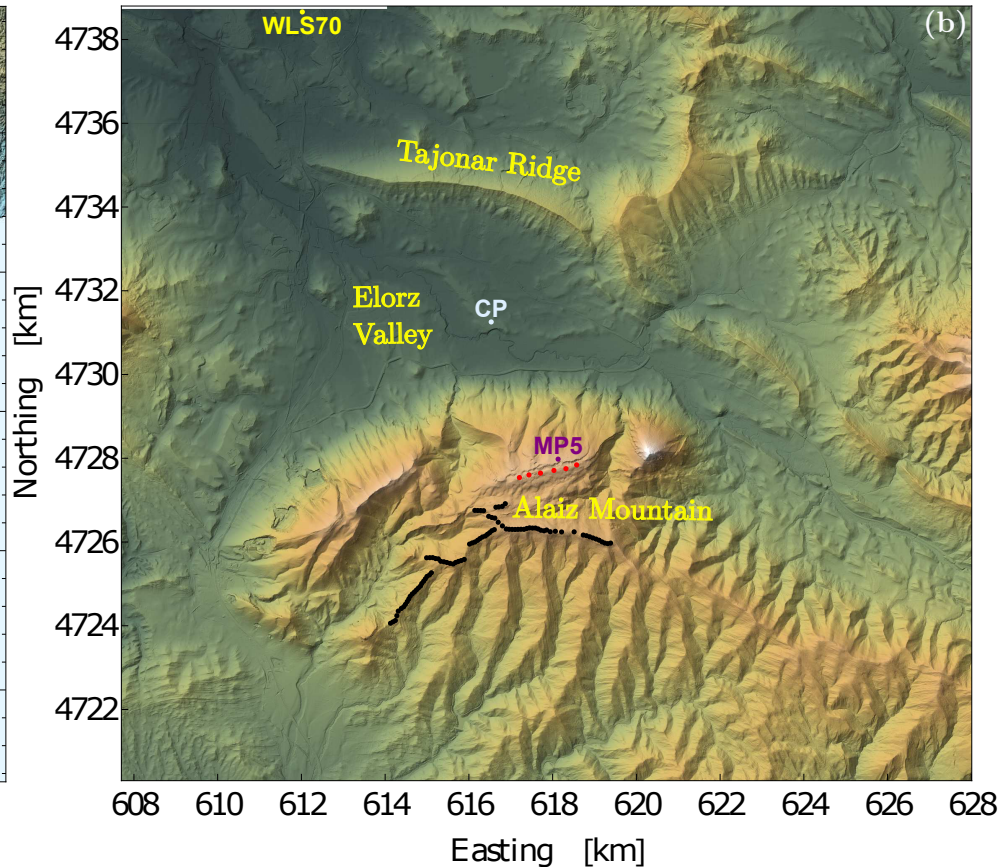
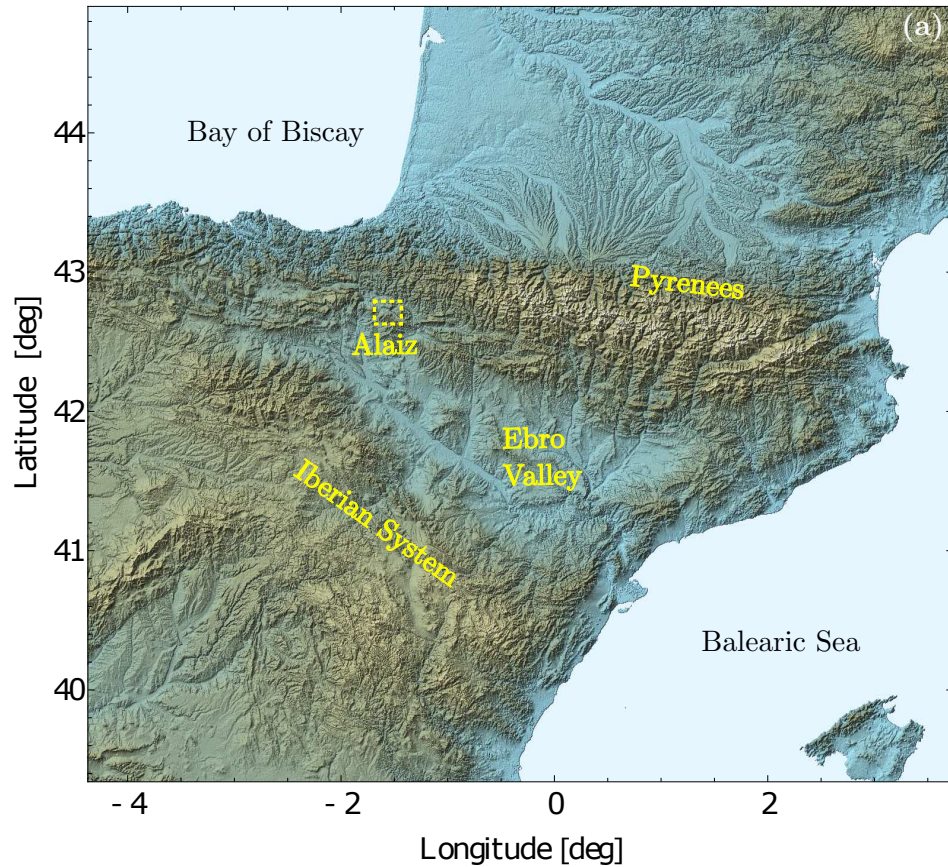
- A multi-scale numerical weather prediction model **simulates** atmospheric hydraulic jumps with similar timing and flow properties as those observed by a multi-lidar setup

Hypothesis 3:

- The vector of vertical flux of horizontal momentum and that of the mean vertical gradient of horizontal wind speed **are aligned** above the atmospheric surface layer.

The Alaiz experiment (ALEX17)

- A large-scale domain (20x20 km) with a mountain-valley-ridge configuration



The Alaiz experiment (ALEX17)



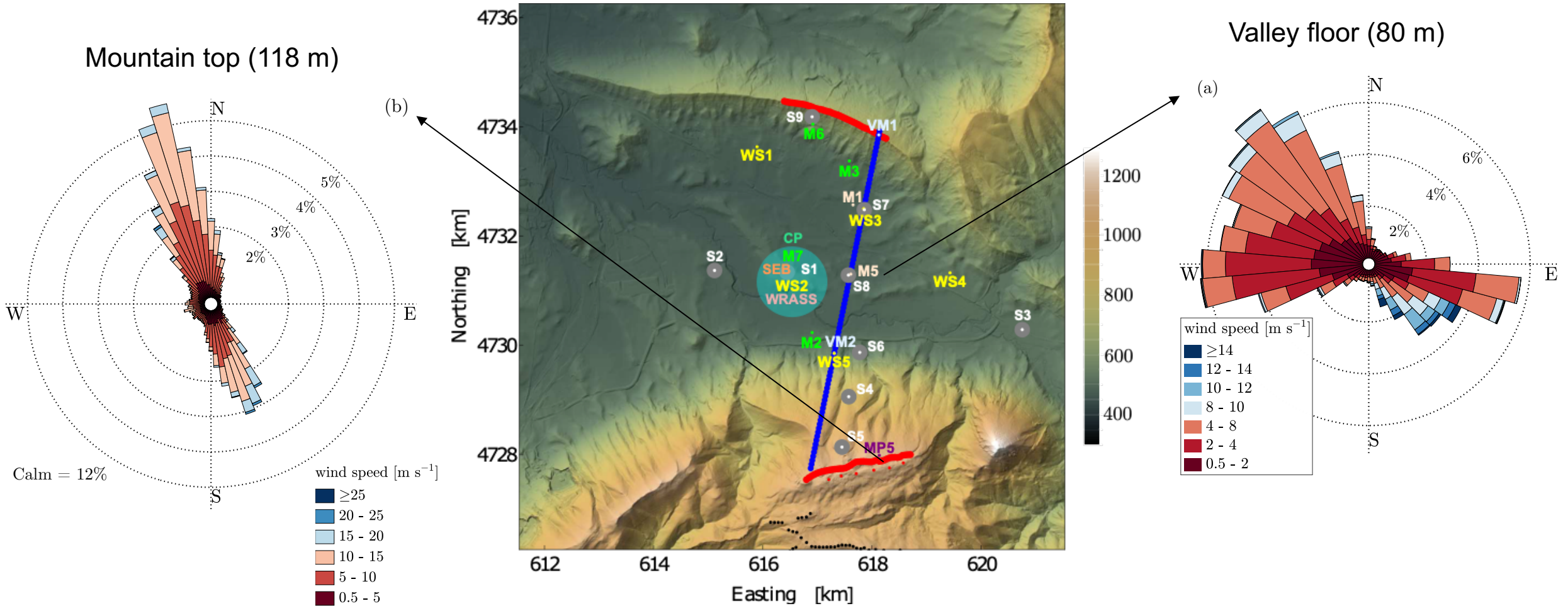
- Observational campaign: May/2018 to Jan/2019



View of the Alaiz mountain towards SE from Tajonar ridge

The Alaiz experiment (ALEX17)

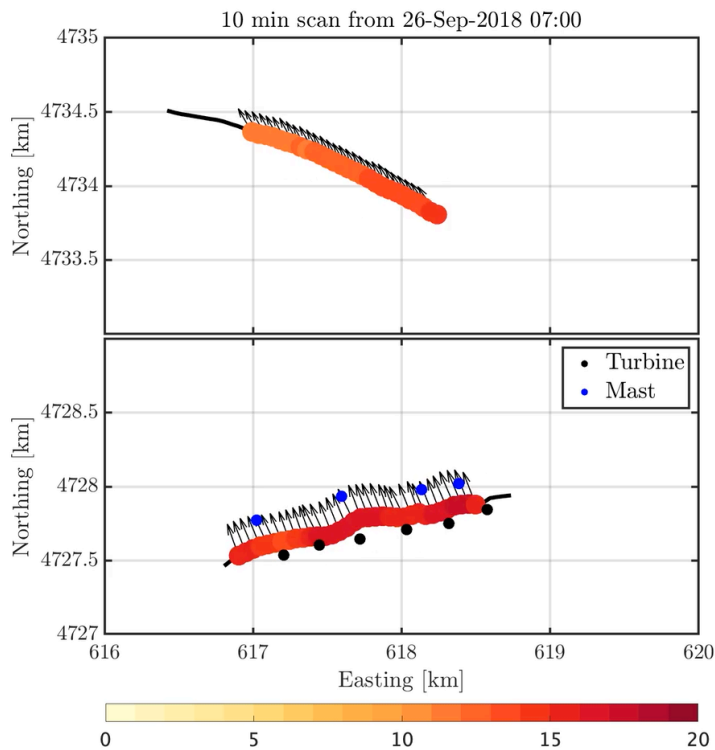
- A large-scale domain (20x20 km) with a mountain-valley-ridge configuration



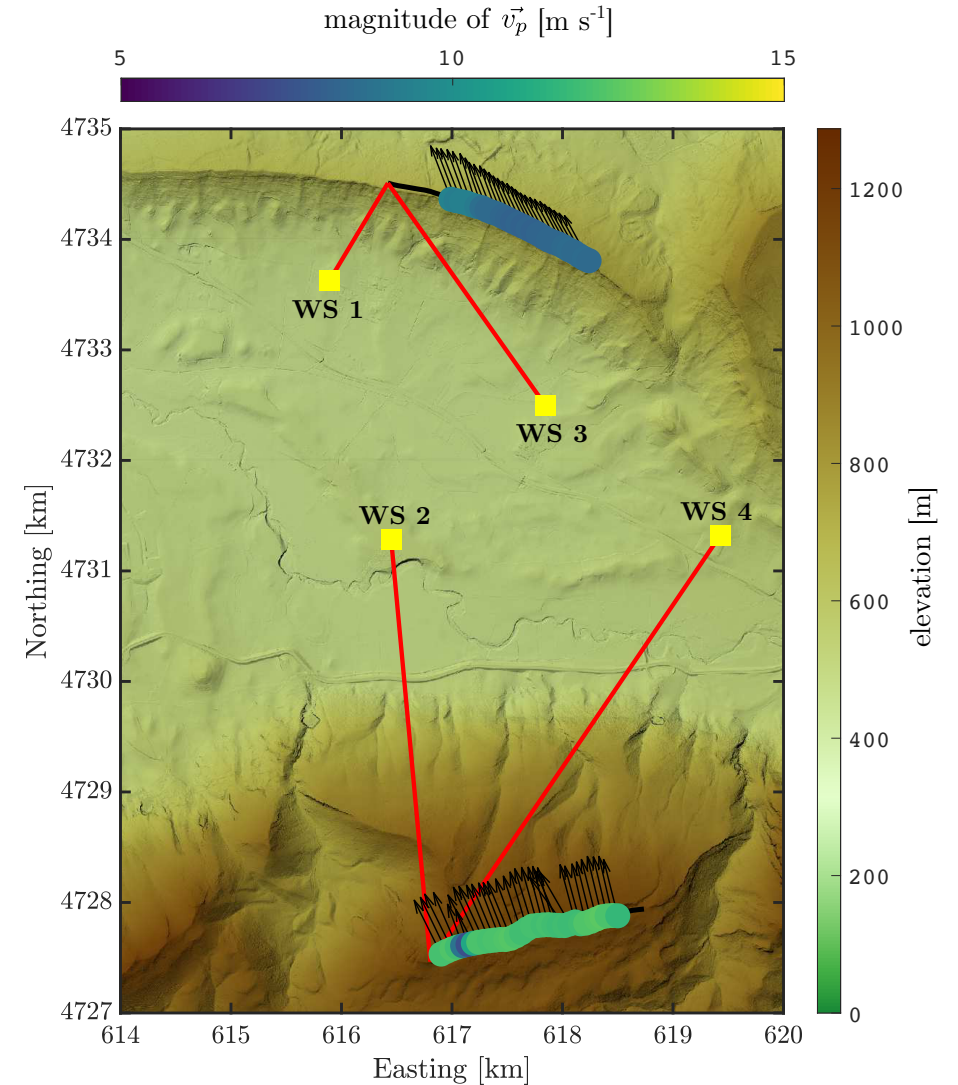
The Alaiz experiment (ALEX17)



- Dual-Doppler along the Alaiz mountain & Tajonar ridge:
 - Recovery for 3-full months: 75.2% at the ridge, 30% at the mountain.

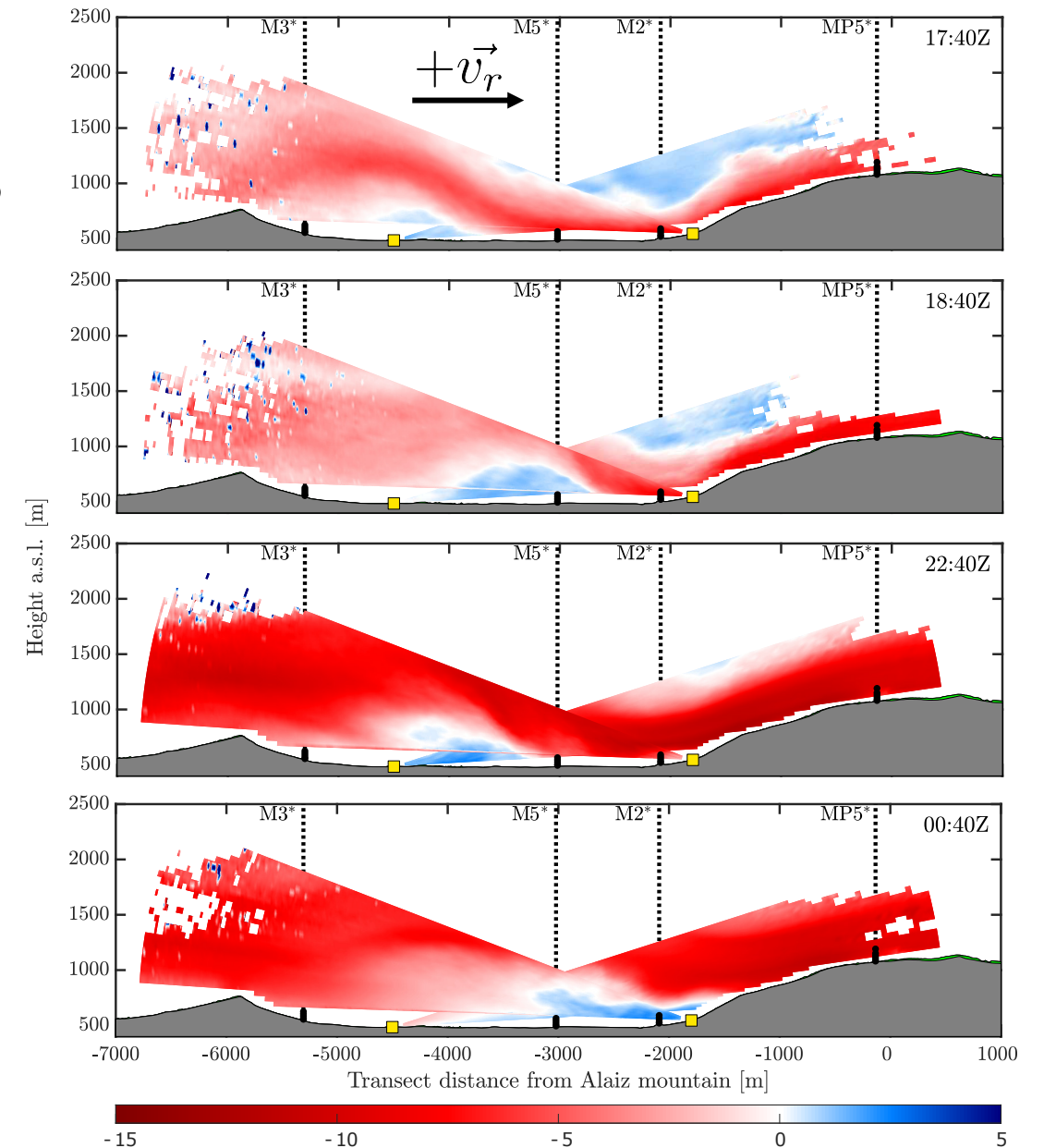


Source: <http://doi.org/10.11583/DTU.13003184>



A hydraulic jump at Alaiz

- Observations between Oct 5th – Oct 6th 2018

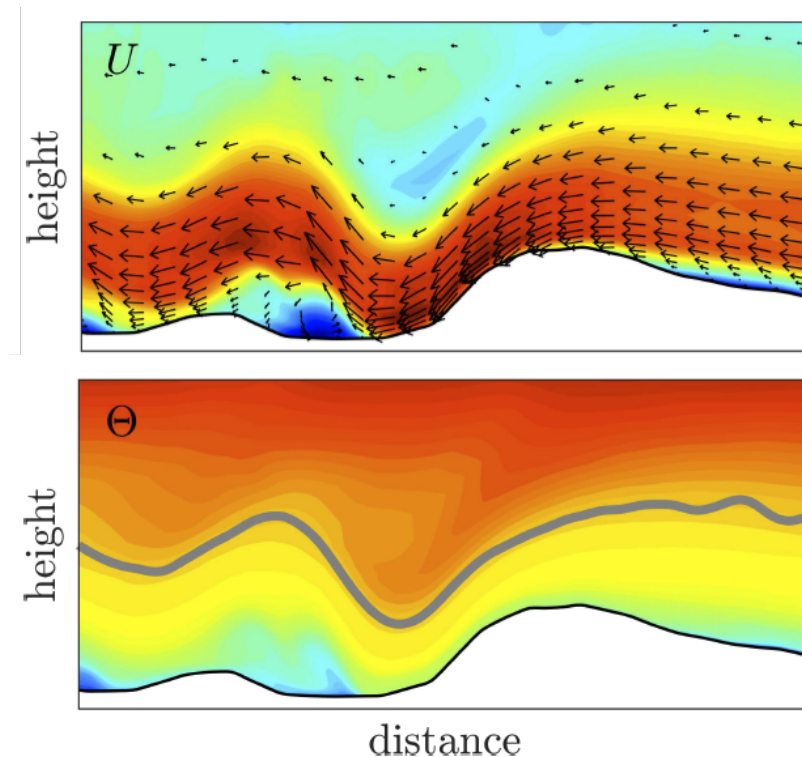


What characterizes a hydraulic jump?

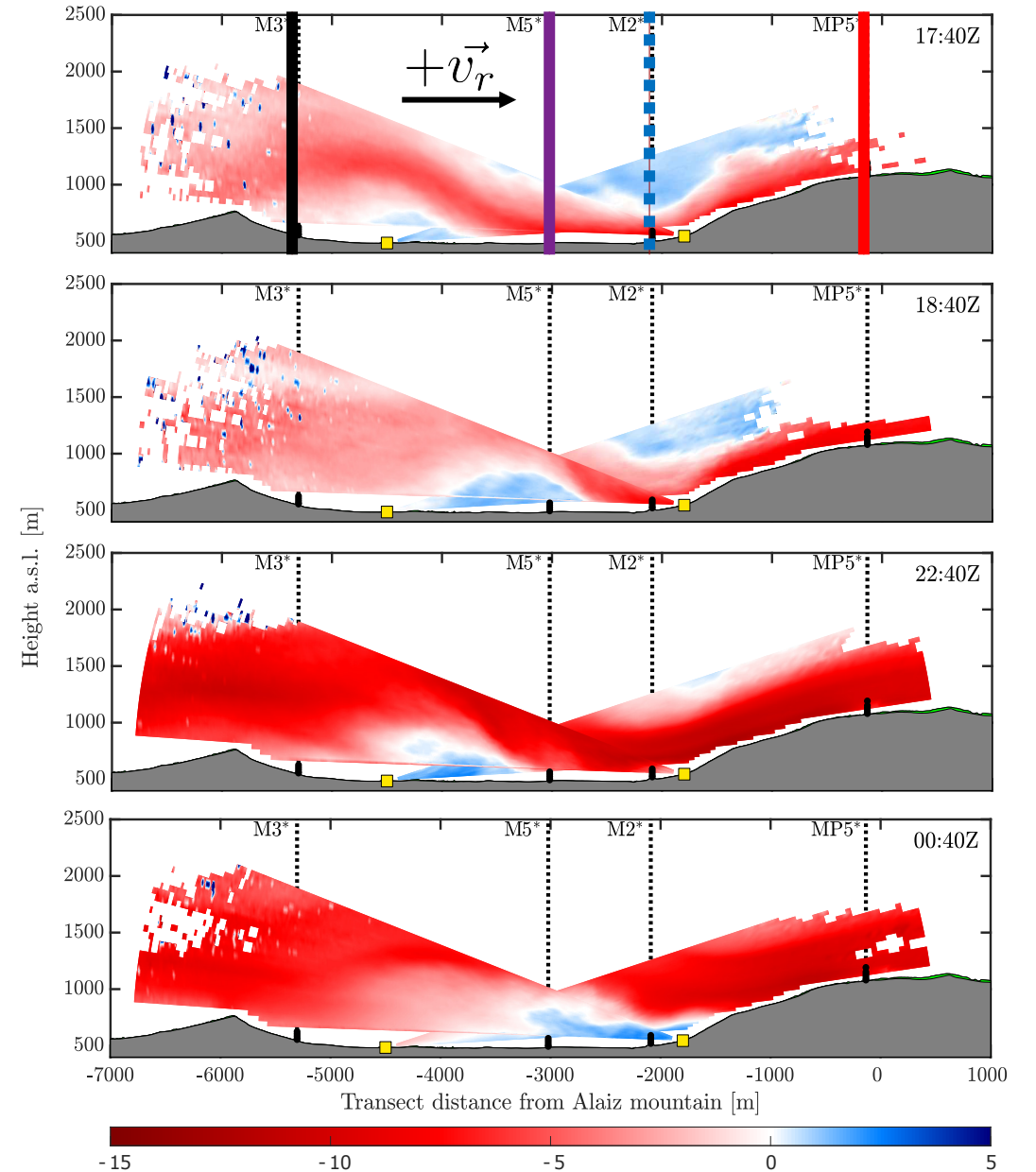
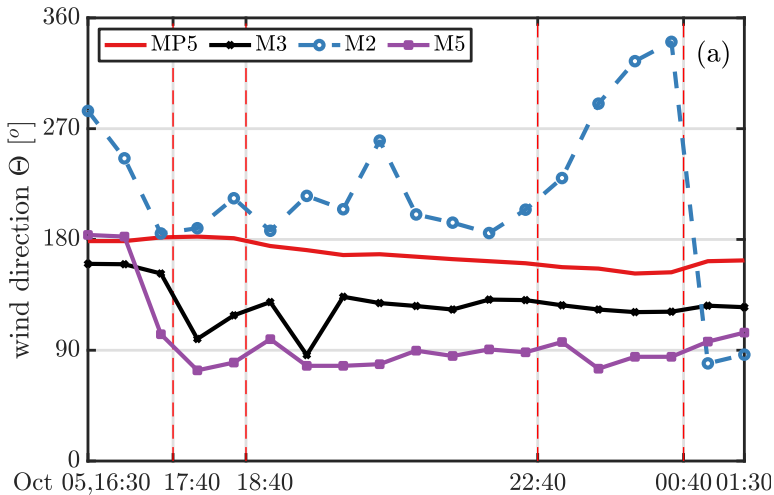
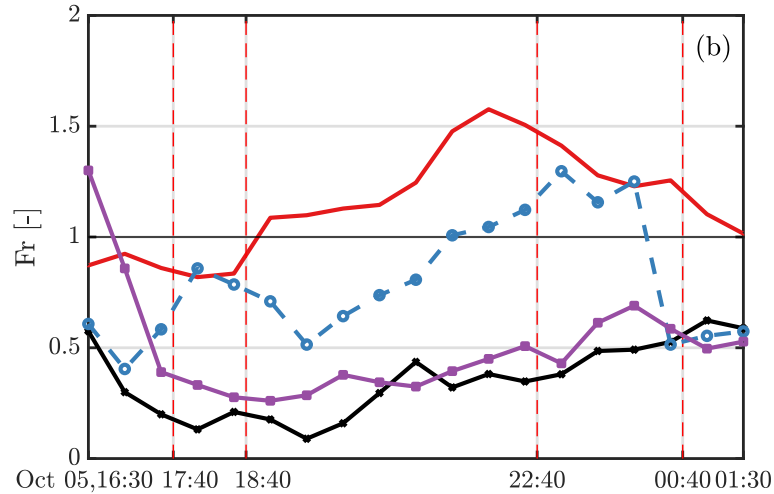
- A hydraulic jump can be interpreted as a flow discontinuity with dissipation of turbulence.
- Long (1954) showed that a Froude transition, i.e. from supercritical (>1) to subcritical (<1), might trigger an atmospheric hydraulic jump

$$Fr_L = \frac{U}{NL}$$

$$N = \sqrt{\frac{g \partial \bar{\theta}}{\bar{\theta} \partial z}}$$



A hydraulic jump at Alaiz – Froude transition

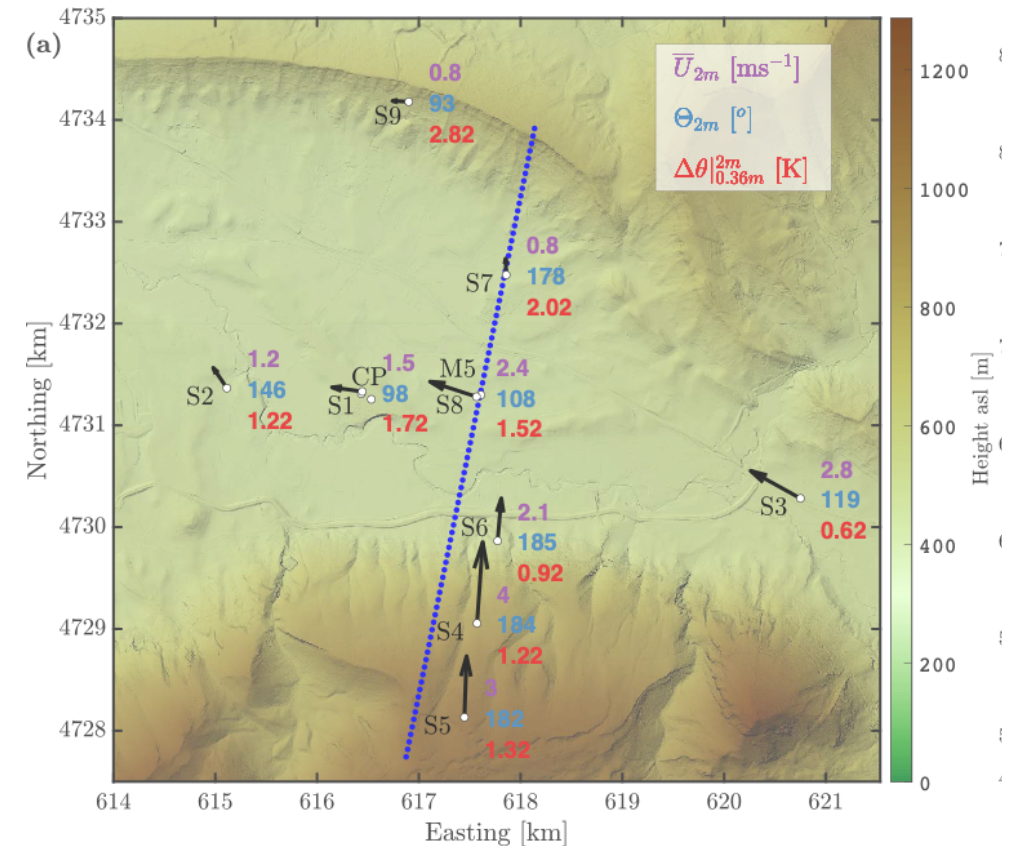


A hydraulic jump at Alaiz – how often does this happen?

- The surface stations show the horizontal distribution of the hydraulic jump phenomenon, with a funnel effect in the valley.

This is a single case, how often does this happen?

- Measurements over a 1-year period show that the Froude number transition for southerly winds happens $\approx 10\%$ of the time.

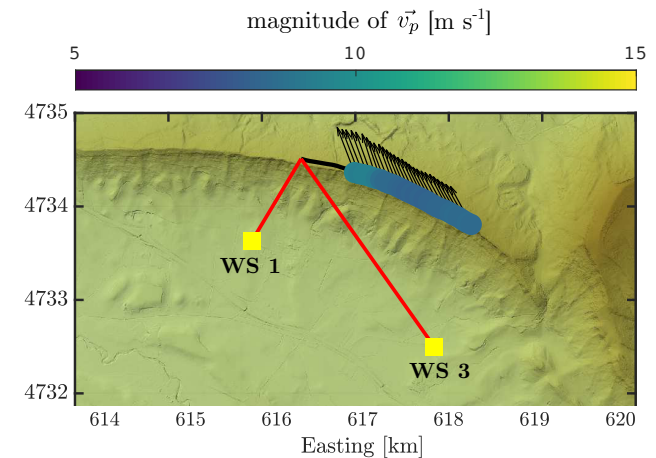
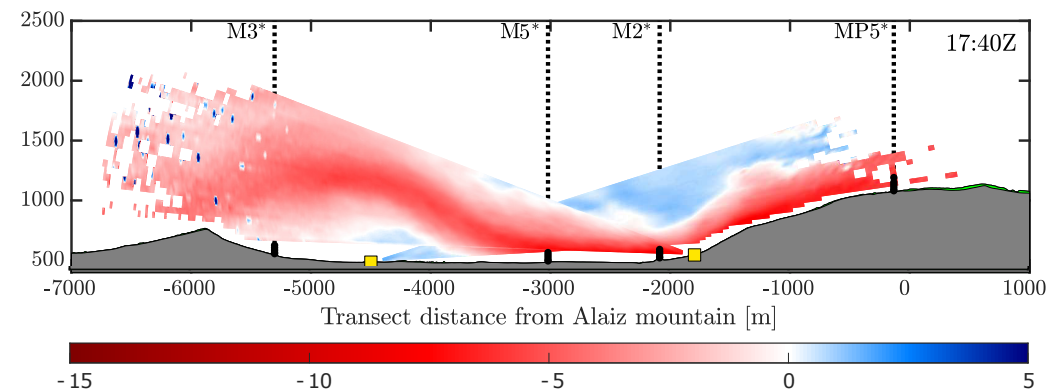


A hydraulic jump at Alaiz – measurement results

- Hypothesis 1 is not falsified

Hypothesis 1:

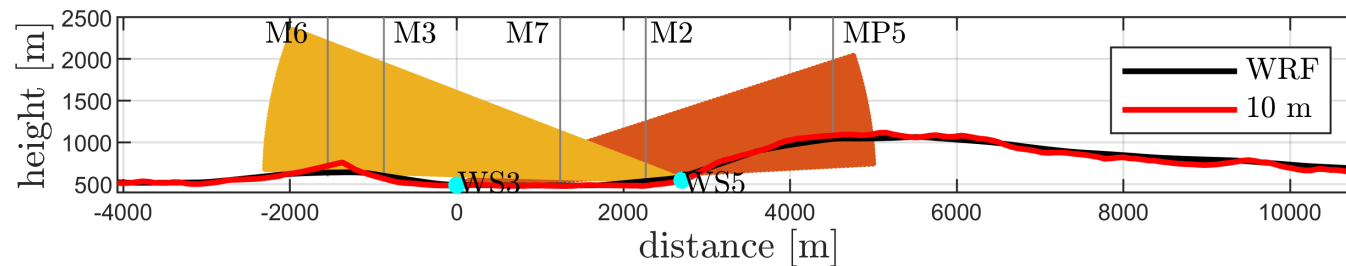
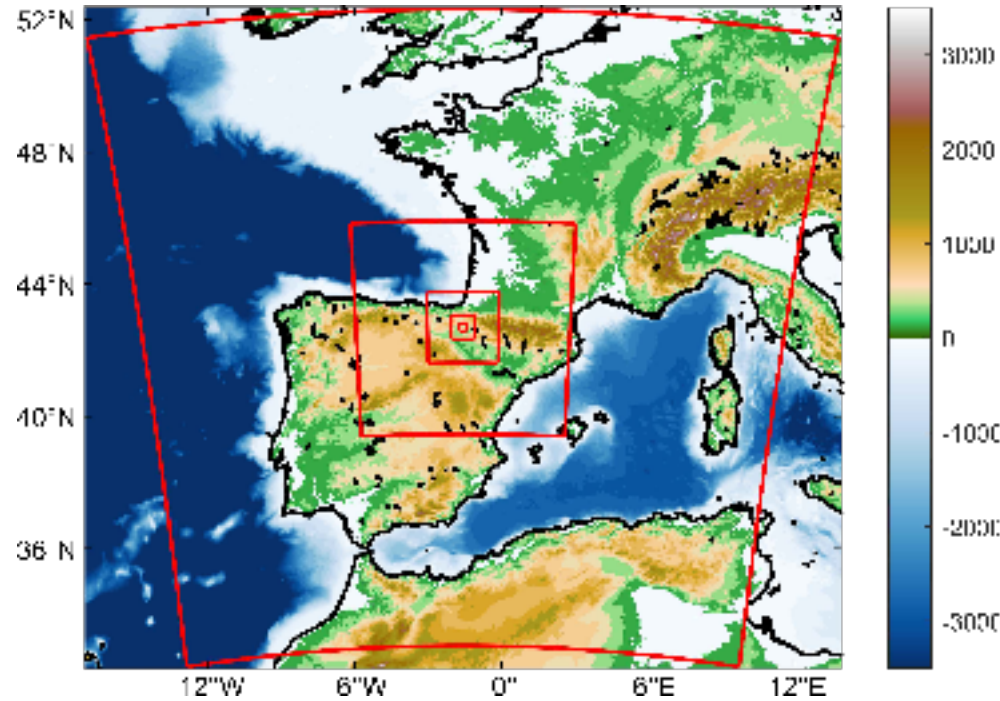
- Multi-lidar measurements of the mean wind flow **portray** flow patterns of different scales, such as atmospheric mountain waves and recirculation zones with features from 100 m and 10 km in mountainous terrain
- Results are published in Wind Energy Science, Santos et al. ([2020](#))



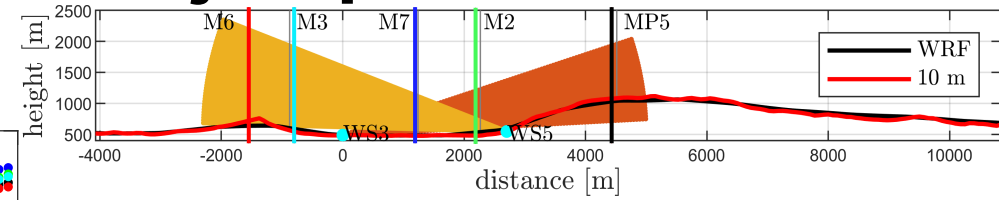
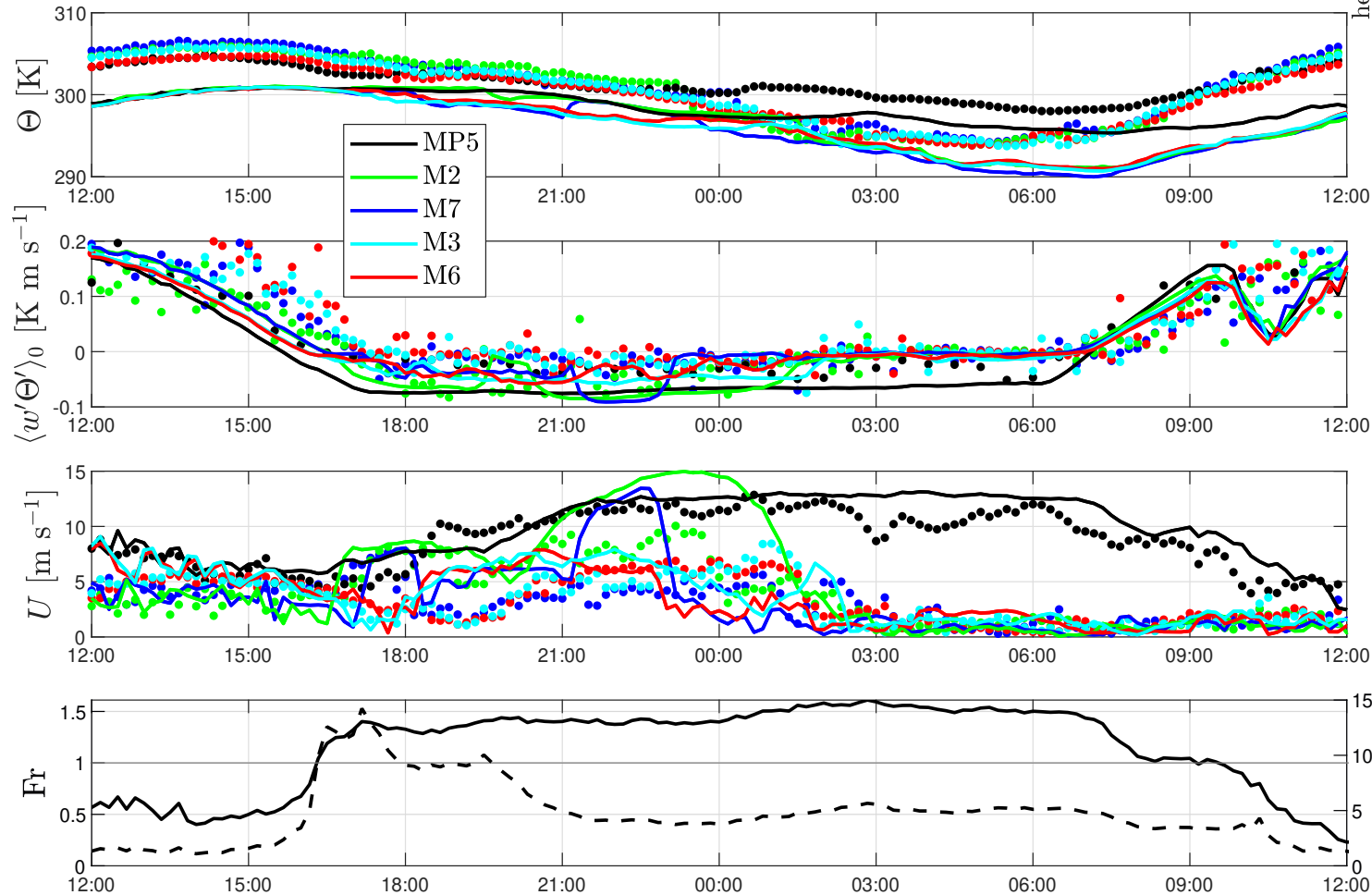
How does these results compare with state-of-the-art numerical models?

Numerical simulations of hydraulic jump and mountain waves

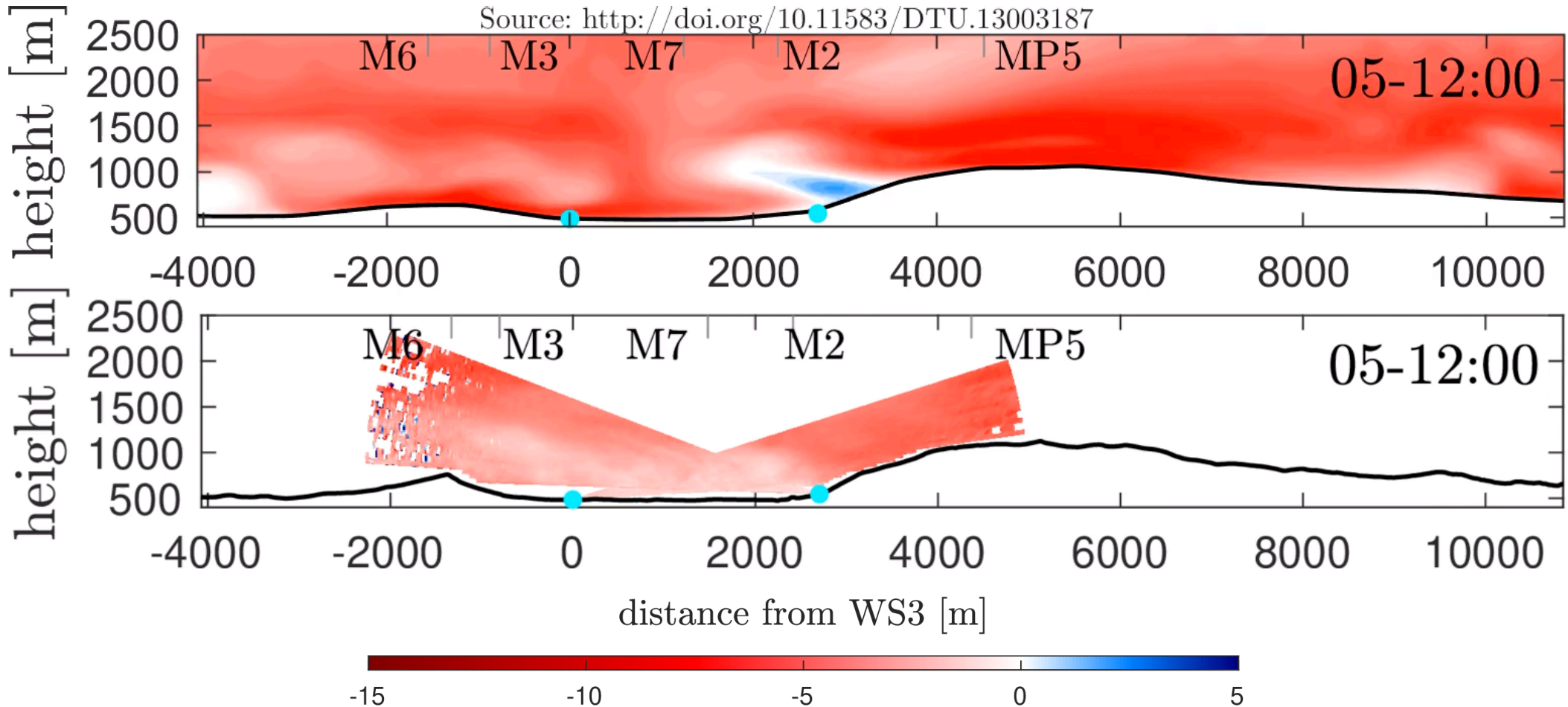
- WRF 4.0.1 simulation conducted by A. Peña



Numerical simulations of hydraulic jump and mountain waves



Numerical simulations of hydraulic jump and mountain waves



Numerical simulations of hydraulic jump and mountain waves

- WRF simulations simulated the atmospheric hydraulic jump with similar timing and flow structures
- Meteorological observations show both agreements and mismatches with simulations.
- Simulations point that both the hydraulic jump and mountain waves occur under supercritical Froude

This is one case, are such results robust?

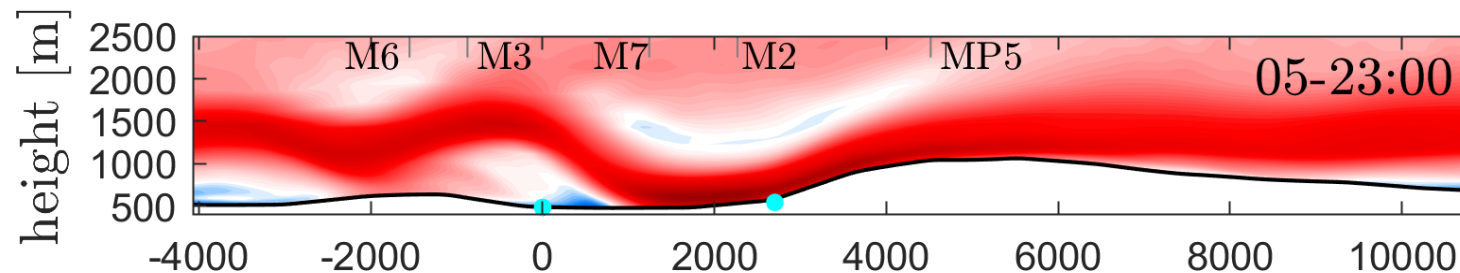
- Four other hydraulic jump cases were identified using the multi-lidar scans
 - All cases also with strong ($> 5 \text{ ms}^{-1}$) and southerly winds at the mountain top with a Froude number transition at the valley.
- Other observed episodes can be the focus of further studies.

Numerical simulations of hydraulic jump and mountain waves

- Hypothesis 2 is not falsified

Hypothesis 2:

- A multi-scale numerical weather prediction model **simulates** atmospheric hydraulic jumps with similar timing and flow properties as those observed by a multi-lidar setup
- Results are published in JGR Atmospheres, Peña and Santos ([2021](#))



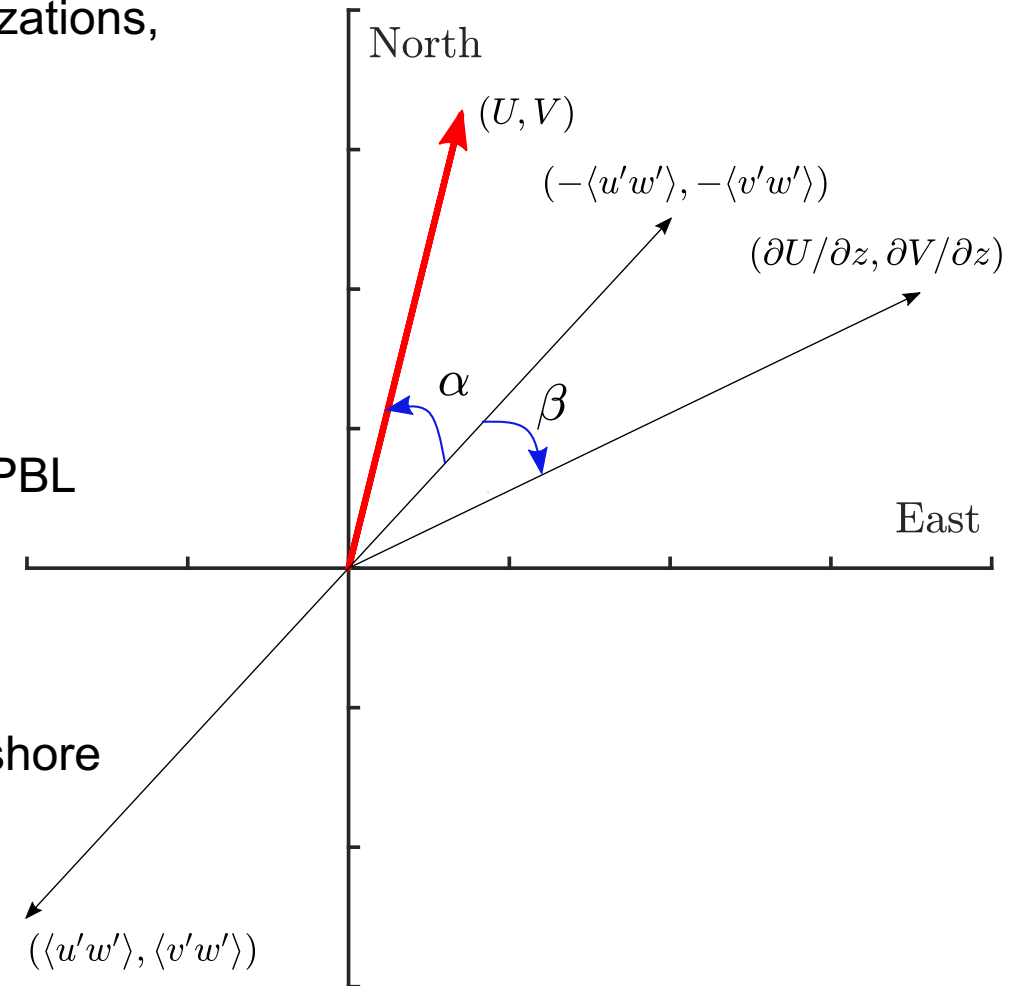
How to use lidar observations to better understand numerical model capabilities?

K-theory departure from PBL - hypothesis

- **Objective:** Evaluate assumption used in PBL parameterizations, common in numerical weather models
- Local PBL schemes in mesoscale models express the momentum fluxes as

$$\overline{u'_i w'} = -K_m \frac{\partial U_i}{\partial z}$$

- Considering this K-theory hypothesis, $\beta = 0^\circ$ across the PBL
- Using NEWA-WRF and a long-range profiling lidar
 - What is the validity of the K-theory hypothesis both onshore and offshore?



K-theory departure from PBL - methodology

• Observations

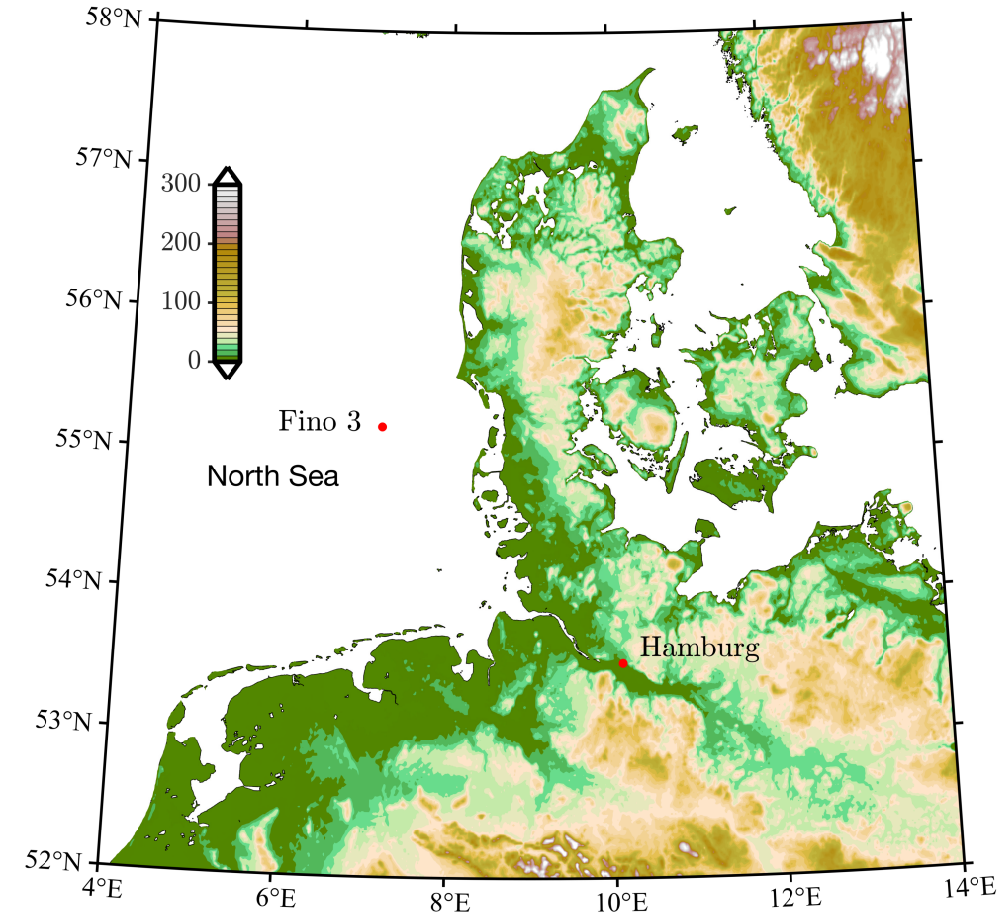
- 1-yr at FINO3 and 3-months at Hamburg
- Valid 30-min lidar data from 100 m to 500 m
- Final time series \equiv valid lidar \cap WRF data
- Momentum flux from lidars:

$$\begin{pmatrix} \langle u'w' \rangle \\ \langle v'w' \rangle \end{pmatrix} = \frac{1}{2 \sin 2\phi} \begin{pmatrix} \sigma^2(v_{r,E}) - \sigma^2(v_{r,W}) \\ \sigma^2(v_{r,N}) - \sigma^2(v_{r,S}) \end{pmatrix}$$

• Numerical model (NEWA-WRF)

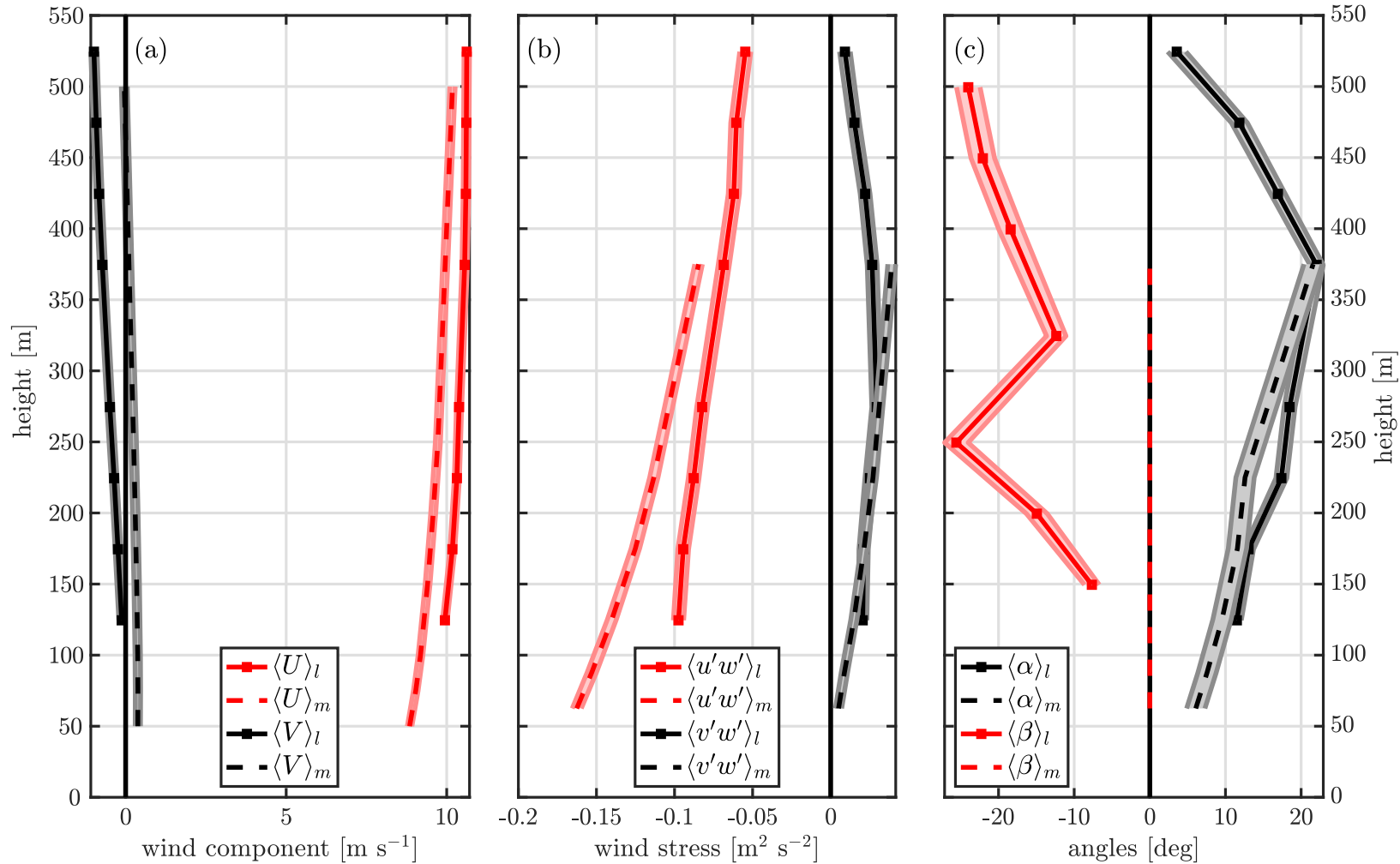
- 30-min time series at FINO3 and Hamburg
- Mellor-Yamada-Nakanishi-Niino level 2.5 is used, i.e.

$$-\overline{u'_i w'} = l \sqrt{2eS} \partial U_i / \partial z$$



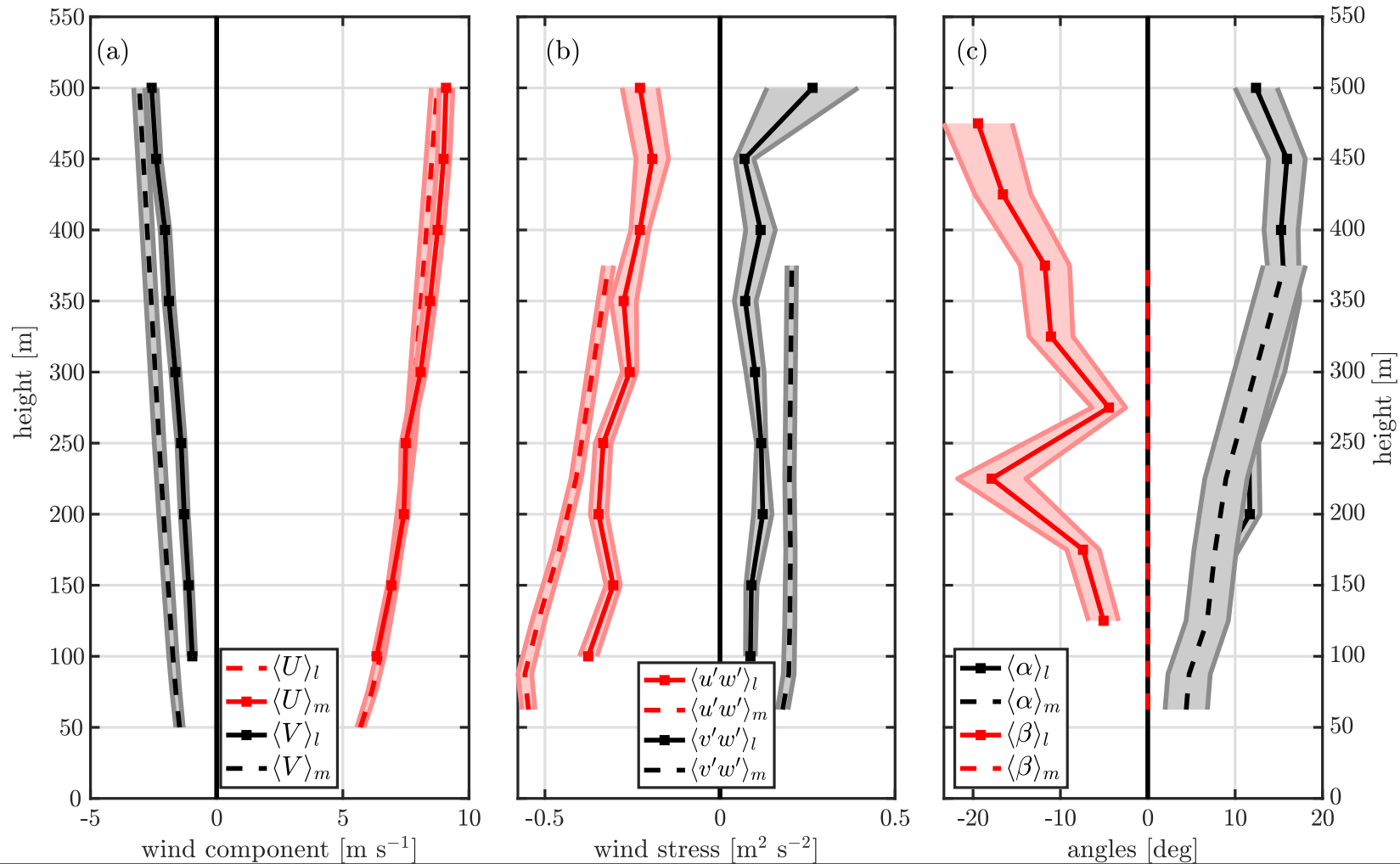
K-theory departure from PBL – offshore results

- Offshore profiles from WRF vs. Lidar from $270^\circ \pm 45^\circ$



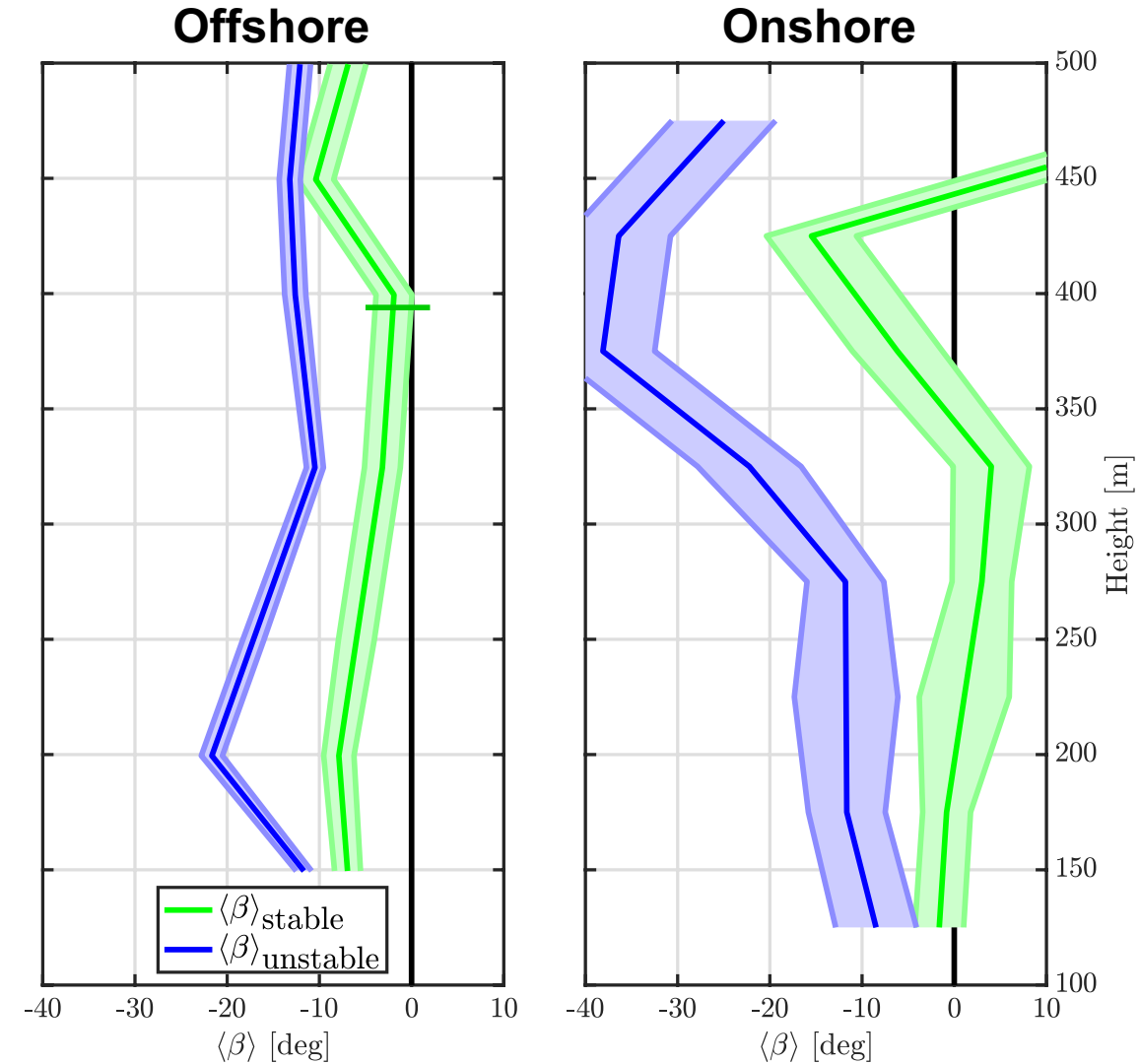
K-theory departure from PBL – onshore results

- Onshore profiles from WRF vs. Lidar from $270^\circ \pm 45^\circ$



K-theory departure from PBL – stability impact

- Strain-stress misalignment as a function of atmospheric stability
- K-theory tends to be valid under stable conditions onshore and on PBL top for offshore conditions



K-theory departure from PBL

- Lidar observations show that between 100-500 m, on average, $\beta \approx -18^\circ$ offshore and $\beta \approx -12^\circ$ onshore
- $\beta = 0^\circ$ assumed by NEWA-WRF **does not** reflect reality
- Hypothesis 3 is falsified

Hypothesis 3:

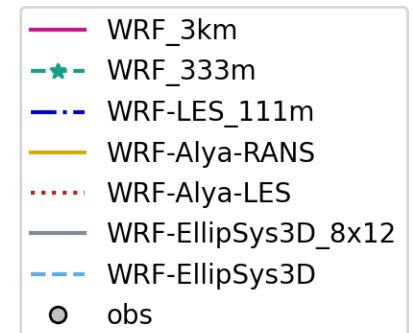
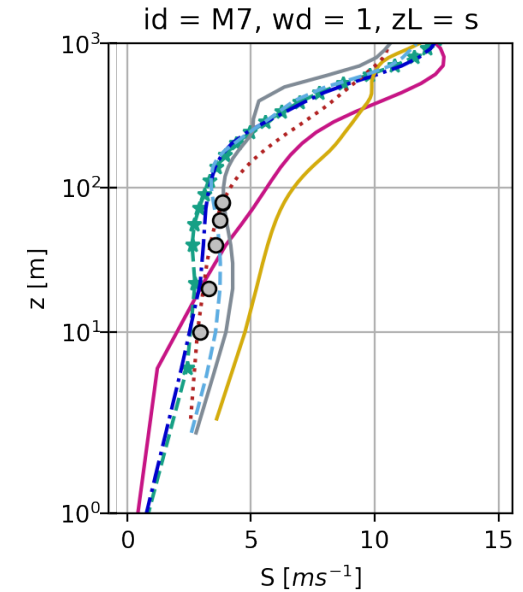
- The vector of vertical flux of horizontal momentum and that of the mean vertical gradient of horizontal wind speed **are aligned** above the atmospheric surface layer.
- Results are under review: Santos, Peña and Mann (in review)

Conclusion

- Alaiz full-scale experiment
 - Full dataset is publicly available, Santos et al. ([2019](#))
 - The multi-lidar transect scan and Dual-Doppler analysis resulted in a flow catalogue for Alaiz
- Hydraulic jump at Alaiz
 - Multi-scanning lidar setup was able to capture flow patterns $O(10 \text{ km})$
 - High-resolution mesoscale simulations match qualitatively the observed hydraulic jump both in time and flow features
 - Froude number analysis and numerical simulation inputs indicate that this phenomenon is frequent and relevant for the studied site
- K-theory departure on PBL
 - First results that indicate stress-strain misalignment both onshore and offshore above the ASL
 - Impact of these results in development of PBL schemes

Outlook

- Further advancement of multi-lidar campaigns
- New dataset for model evaluation and validation
 - Two numerical model benchmarks are ongoing (IEA Task 31)
- First step towards time-resolved numerical modelling at Alaiz
 - More studies on the hydraulic jump are being performed (WESC 2021)
- Stress-strain misalignment to be connected with atmospheric processes (e.g. cloud formation)



Thank you for the attention!
Obrigado!
Tusind tak!

